A QUANTITATIVE EVALUATION METHOD BASED ON EMD FOR DETERMINING THE ACCURACY OF TIME-VARYING SEISMIC WAVELET EXTRACTION

PENG ZHANG, YONGSHOU DAI, RONGRONG WANG and YONGCHENG TAN

College of Information and Control Engineering, China University of Petroleum (East China), Qingdao 266580, P.R. China. upczhangpeng@163.com

(Received September 29, 2016; revised version accepted March 29, 2017)

ABSTRACT

Zhang, P., Dai, Y., Wang, R. and Tan, Y., 2017. A quantitative evaluation method based on EMD for determining the accuracy of time-varying seismic wavelet extraction. *Journal of Seismic Exploration*, 26: 267-292.

The bandwidth and amplitude of wavelet deconvolution results are the most important indicators of accuracy for time-varying wavelets. To evaluate the accuracies of extracted seismic wavelets based on these indicators, we propose a quantitative evaluation method based on empirical mode decomposition (EMD), which offers the advantages of adaptive decomposition and multi-scale analysis and can highlight local characteristics. First, time-varying seismic wavelets are extracted from a non-stationary seismogram and subjected to deconvolution or reflectivity inversion. Then, to appraise these wavelets, the amplitude spectrum from the deconvolution or inversion results is decomposed into multi-layer intrinsic mode functions (IMF) using EMD. Next, an evaluation parameter is constructed by summing the number of local extremes in all IMFs and normalizing this sum with respect to the number of frequency points in the amplitude spectrum. Larger values of this parameter indicate more accurate extracted wavelets. When applied to both synthetic and field-collected seismic data, the proposed method performs better than conventional methods for evaluating the accuracy of time-varying wavelet extraction.

KEY WORDS: time-varying wavelet extraction, accuracy evaluation, deconvolution, EMD.

INTRODUCTION

Seismic wavelet extraction is important for seismic data deconvolution, wave impedance inversion and forward modeling, and the precision of the extraction results affects the reliability and accuracy of subsequent seismic data processing and interpretation. In real seismic data, seismic wavelets are scattered from and absorbed by the underground medium during propagation, resulting in a lack of high-frequency components and causing phase distortion

0963-0651/17/$5.00

of the wavelets (van der Baan, 2008; Li et al., 2015). The bandwidth, energy and phase characteristics of time-varying seismic wavelets strongly affect the resolution of seismic data, and the accurate extraction of time-varying seismic wavelets has therefore become a popular area of research on seismic data processing. In recent years, researchers have proposed various improved methods of extracting time-varying wavelets, such as adaptive segmentation (Wang et al., 2012) and time-frequency spectral modeling (Dai et al., 2015). Meanwhile, reasonable and effective methods for evaluating wavelet accuracy, which are important for enabling the selection of accurate wavelets for application and for improving the efficiency of seismic data processing, have also been studied.

Direct and indirect evaluation are two methods that are currently used to evaluate the accuracy of seismic wavelets. Direct methods include the following two approaches: evaluating the accuracy of wavelets according to their own properties (Rietsch, 1997), such as wavelength and energy, and evaluating wavelet accuracy based on logged data (Arild and Henning, 2003). However, both of these methods have distinct disadvantages in practical applications; specifically, it is difficult to apply the rough evaluations offered by the first method for real data processing, and the second method is too strongly relied on. Indirect methods also include two approaches. First, the synthetic seismogram obtained from an extracted wavelet can be compared with the real data (Chen et al., 2013); however, the reflectivity sequence from the logged data must be known a priori, and large errors arise when noise is present. Second, because it is universally acknowledged that the bandwidth and energy of the time-varying wavelet deconvolution results for non-stationary seismograms indicate the accuracy of the wavelets (Sajid and Ghosh, 2013; Oliveira and Lupinacci, 2013), extracted wavelets can be qualitatively evaluated based on their deconvolution results; however, this method is merely intuitive, not quantitative. Although several evaluation criteria, such as the parsimony and Kurtosis criteria (Yuan and Wang, 2011), have been used for quantitatively evaluating residual phase correction, this method can only be applied when the data contain limited extreme values, and it is difficult to effectively evaluate the bandwidth and energy in the frequency domain. Moreover, the evaluation capability of the method severely decreases when it is used for time-varying deconvolution to suppress the time-varying nature of the wavelets and improve the resolution of the seismic data.

To compensate for the deficiencies of existing methods in evaluating the bandwidth and energy in the frequency domain, an indirect and quantitative evaluation method based on empirical mode decomposition (EMD) is proposed to more effectively evaluate the accuracy of extracted time-varying seismic wavelets. The theoretical basis of the proposed method is that the bandwidth and energy of the amplitude spectrum obtained through the deconvolution or reflectivity inversion of extracted wavelets can indirectly reflect the accuracy of

time-varying wavelets. The highly oscillatory behavior of the amplitude spectrum of a seismogram directly reflects the bandwidth and energy, and EMD is a suitable means of analyzing this oscillatory behavior because it provides the capability of adaptive decomposition. Based on the observed characteristics of the amplitude spectrum, an evaluation parameter can be constructed to quantitatively and intuitively express the evaluation results, and this method can be used to effectively evaluate the accuracy of time-varying wavelets regardless of whether they are subjected to deconvolution or reflectivity inversion. Therefore, in contrast to conventional evaluation methods based on qualitative analysis and evaluation criteria, the proposed method offers a superior ability to evaluate bandwidth and energy in the frequency domain based on the construction of a reasonable evaluation index and behaves well in the presence of noise. A flow chart of the proposed method is shown in Fig. 1.

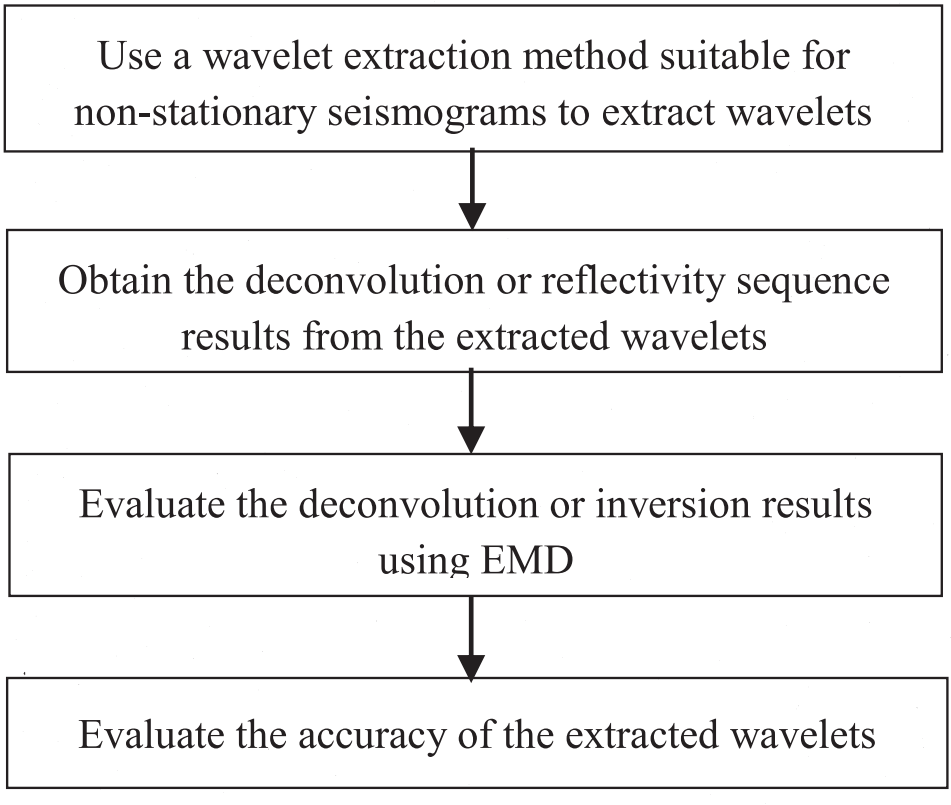

Fig. 1. Flow chart of the proposed evaluation method based on EMD.

WAVELET ACCURACY EVALUATION METHOD BASED ON EMD

The proposed method is an indirect evaluation method that allows the wavelet accuracy to be evaluated by using EMD to obtain the bandwidth and energy from the results of time-varying deconvolution or reflectivity inversion based on time-varying seismic wavelets. One method of extracting such wavelets is time-frequency spectral modeling, which is the method considered in this paper.

Time-varying wavelet extraction based on time-frequency spectral modeling

The non-stationary convolutional model of a seismic trace is often defined as follows (Margrave et al., 2011):

$$x(t) = \int_{-\infty}^{\infty} w(t-\tau,\tau)r(\tau)d\tau = w(t,\tau) * r(t) \quad , \tag{1}$$

where $*$ represents convolution; $x(t)$ is the non-stationary seismogram; $r(t)$ is the reflectivity; and $w(t,\tau)$ is the function describing the wavelet, which allows temporal evolution and simple delay.

In the time-frequency spectral modeling method, it is assumed that the amplitude and high-frequency component vary with time and that the wavelet phase is time-invariant. The improved generalized S transform is used to transform a non-stationary seismogram from the time domain into the time-frequency domain (Zhang et al., 2011; Radad et al., 2015). The window function for this transform is

$$G(t,f) = [1/\sqrt{(2\pi)}q|f|^{p}]\exp(-t^2/2q^2f^{2p}) \quad , \tag{2}$$

where q and p are adjustment factors that are greater than zero. The time-frequency spectrum of the signal $x(t)$ is expressed as follows:

$$X(\tau,f) = \int_{-\infty}^{\infty} x(t)G(t-\tau,f) \times \exp(-i2\pi ft)dt \quad , \quad f \neq 0, \tag{3}$$

where τ is the sample time. Considering the time-frequency transform, a high time resolution is observed at high frequencies and a high frequency resolution is observed at low frequencies, which conforms to the dynamic attenuation characteristics of the seismogram.

By fixing t, the amplitude spectrum X(t,f) can be obtained for the corresponding instant of time, and the time-varying seismic wavelets can then be estimated from the wavelet amplitude spectra extracted for all instants of time via spectral modeling and from the wavelet phase spectra via the bispectrum method based on higher-order cumulants.

Spectral modeling assumes that the wavelet amplitude spectrum is smooth and similar to the unimodal curve of the Ricker wavelet spectrum and that the amplitude spectrum of the reflectivity sequence is oscillating at a high frequency (Rosa and Ulrych, 1991; Economou et al., 2010). The empirical mathematical expression for a seismic wavelet is as follows:

$$W(f) = |f|^k \exp\left(\sum_{n=0}^{N} a_n f^n\right) , \tag{4}$$

where k is a constant, a_n are the coefficients of the polynomial in f, and N is the order. Using this expression, the least-squares method can be applied to obtain the wavelet amplitude spectrum from the seismogram. The wavelet amplitude spectrum at each point can thus be extracted via spectral modeling combined with time-frequency analysis.

Next, the phase of the seismic wavelet must be extracted using the Matsuora-Ulrych algorithm (Matsuoka and Ulrych, 1984). The third-order cumulants of the seismogram can be expressed as follows:

$$c_x(\tau_1,\tau_2) = E[x(t)x(t + \tau_1)x(t + \tau_2)] . \tag{5}$$

After performing a Fourier transform, we obtain the third-order spectrum of x(t), i.e., the bispectrum, with the following amplitude and phase spectra:

$$|B_x(\omega_1,\omega_2)| = |X(\omega_1)||X(\omega_2)||X(\omega_1 + \omega_2)| , \tag{6}$$

$$\psi(\omega_1,\omega_2) = \phi(\omega_1) + \phi(\omega_2) - \phi(\omega_1 + \omega_2) , \tag{7}$$

where $\phi(\omega)$ is the phase spectrum of x(t) and $|X(\omega)|$ is the amplitude spectrum.

Based on the convolutional model and the nature of the bispectrum, the following equation is obtained:

$$B_x(\omega_1,\omega_2) = B_r(\omega_1,\omega_2) + B_\omega(\omega_1,\omega_2) , \tag{8}$$

where $B_r(\omega_1,\omega_2) = \sigma^2$. The wavelet bispectrum and the seismogram bispectrum are related by a coefficient of proportionality, which allows us to obtain the

wavelet bispectrum from the seismogram bispectrum based on the equation

$$\psi(\omega_1,\omega_2) = \varphi(\omega_1) + \varphi(\omega_2) - \varphi(\omega_1 + \omega_2) \quad , \tag{9}$$

where $\varphi(\omega)$ is the phase spectrum of the seismic wavelet and the wavelet spectrum at each sample is expressed as follows:

$$\tilde{\omega}(\tau,t) = F^{-1}\{|W(\tau,\omega)|\exp[j\varphi(\omega)]\} \quad , \tag{10}$$

where $\tilde{\omega}(\tau,t)$ represents the extracted time-varying wavelet and F^{-1} represents the inverse Fourier transform.

Time-varying deconvolution

Time-varying wavelet deconvolution is conducted for the following two reasons.

To compensate for energy attenuation and improve the resolution of seismic data, the deconvolution factor can be constructed as follows using a time-varying wavelet (Zhou et al., 2014):

$$O(\tau,f) = \begin{cases} A_{max}/[|W(\tau,f)| + \varepsilon * A_{max}] & , \quad f_b < f < f_c \\ 1 & , \quad f < f_a \text{ or } f > f_d \\ 1 + (\lambda * A_{max})/[|W(\tau,f)| + \varepsilon * A_{max}] - \lambda & , \quad \text{else} \end{cases} \tag{11}$$

where $A_{max} = \max\{|W(\tau,f)|\}$; $0 \le \lambda \le 1$; $0.005 \le \varepsilon \le 0.05$; f_a, f_b, f_c and f_d are the control parameters; and $f_a < f_b < f_c < f_d$. The deconvolution result is as follows:

$$R(t) = \int_{-\infty}^{\infty}\int_{-\infty}^{\infty} X(\tau,f)O(\tau,f)\exp(i2\pi ft)dtdf \quad . \tag{12}$$

Time-varying seismic wavelets can be subjected to reflectivity inversion to provide references for seismic interpretation (Porsani et al., 2013). The most effective method is to combine the methods of time-frequency spectral modeling deconvolution and nonlinear sparse deconvolution (Sun et al., 2015). The time-varying nature of the wavelets is initially suppressed, such that the non-stationary seismogram becomes stationary. Then, the nonlinear method is applied to obtain the precise inversion of the reflectivity sequence.

Sparse deconvolution can be applied to invert the reflectivity sequence by using the basic principle of Bayesian sparse inversion (Velis, 2008; Sun et al., 2015). The convolutional model of a seismogram can be expressed in vector form as follows:

$$\mathbf{s} = \mathbf{C}_\omega \mathbf{r} + \mathbf{n} \quad , \tag{13}$$

where $\mathbf{s} = [s_1, s_2, \mathrm{L}\ , s_N]^T$ represents the seismic observation data; $\mathbf{r} = [r_1, r_2, \mathrm{L}, r_N]^T$ is the reflectivity sequence; $\mathbf{C}_\omega$ is the $N \times M$-dimensional convolutional matrix of wavelets; and $\mathbf{n} = [n_1, n_2, \mathrm{L}\ , n_n]^T$ is the observation noise, which is assumed to obey a normal distribution with a mean of zero and a variance of σ_n^2. The vector form of the objective function based on the Cauchy sparse constraint can be expressed as follows:

$$J_2 = (1/2\sigma_n^2)(\mathbf{C}_\omega \mathbf{r} - \mathbf{s})^T(\mathbf{C}_\omega \mathbf{r} - \mathbf{s}) + \tfrac{1}{2} \left\| \ln[1 + \mathrm{diag}(\mathbf{r})\mathbf{r}/2\sigma_r^2] \right\|_1 \quad . \tag{14}$$

The corresponding regularization equation is as follows:

$$(\mathbf{C}_\omega^T \mathbf{C}_\omega + \mu \mathbf{Q})\mathbf{r} = \mathbf{C}_\omega^T \mathbf{s} \quad , \tag{15}$$

where μ is the experience parameter and $\mathbf{Q}$ is a diagonal matrix that can be expressed as

$$\mathbf{Q} = [1 + \mathrm{diag}(\mathbf{r})\mathbf{r}/2\sigma_r^2] \quad . \tag{16}$$

The steps of inverting the reflectivity sequence using an iterative method are as follows:

1. The initial reflectivity sequence is calculated.

2. The two basic parameters σ_r and σ_n of the Cauchy constraint conditions are chosen.

3. The parameter μ, the diagonal matrix $\mathbf{Q}$ and the correlation matrix $\mathbf{C}_\omega^T \mathbf{C}_\omega$ are calculated to iteratively solve the regularization equation as follows:

$$\mathbf{r}^k = (\mathbf{C}_\omega^T \mathbf{C}_\omega + \mu \mathbf{Q}^{(k-1)})^{-1} \mathbf{C}_\omega^T \mathbf{s} \quad , \tag{17}$$

where k is the iteration.

Evaluation method based on EMD

The proposed evaluation method includes the following steps: obtain the Fourier transform of the deconvolution or inversion result, decompose the

frequency result using EMD and construct the evaluation parameter, and evaluate the accuracy of the extracted time-varying wavelets based on the calculated parameter value.

EMD was proposed by Huang (1998) to decompose a signal into a series of oscillatory modes. Each of these oscillatory modes is represented by an intrinsic mode function (IMF) with the following definition: (1) among the entire dataset, the number of extremes and the number of zero crossings must be equal or differ by no more than one, and (2) the mean value of the envelope defined by the local maxima and the envelope defined by the local minima at any point is zero. Decomposition stops when only a trend component remains (Han and van der Baan, 2013). A signal x(t) that has been decomposed via EMD can be expressed as follows:

$$x(t) = \sum_{i=1}^{N} imf_i(t) + c(t) \quad , \tag{18}$$

where imf_i is the i-th IMF component and c(t) is the residue component.

The amplitude spectrum of a seismogram or a reflectivity sequence is highly oscillatory with a large number of local extremes, and the numbers of oscillation components and local extremes depend on the bandwidth and energy in the frequency domain. If it is assumed that a reflectivity sequence obeys a mixed Gaussian distribution, then its amplitude spectrum is distributed over the entire frequency band. Affected by the time-varying wavelets, the high-frequency components of the spectrum are suppressed in the process of convolution, and compared with those of a reflectivity sequence, the bandwidth and energy of the corresponding seismogram are reduced and the numbers of oscillation components and local extremes are similarly decreased. The time-varying wavelet deconvolution of a non-stationary seismogram is an effective method of broadening the bandwidth and increasing the energy in the frequency domain, thereby improving the resolution, and the bandwidth and energy of the results of deconvolution or inversion are important indicators of the accuracy of the time-varying wavelets (Sajid and Ghosh, 2013; Oliveira and Lupinacci, 2013). Wider frequency bands and higher amplitude energies correspond to more local extremes, more oscillation components and more accurate wavelets.

EMD can be used to analyze and compare the bandwidth and energy of a seismogram before and after time-varying wavelet deconvolution because the adaptive decomposition provided by EMD is able to highlight the oscillatory behavior in each IMF. Wider frequency bands and higher amplitude energies correspond to more local extremes in each IMF. Therefore, the wavelet

accuracy can be indirectly evaluated by counting the number of local extremes in each IMF. The evaluation parameter for the wavelet accuracy can be constructed as follows:

1. The results of deconvolution or inversion are Fourier transformed to obtain the amplitude spectrum, which is regarded as the original signal.

2. To find the local maximum and minimum of the original signal, upper and lower envelopes are obtained by fitting the local extremes.

3. The mean of the upper and lower envelopes is calculated.

4. The mean obtained in step (3) is subtracted from the original signal.

5. The result from step (4) is analyzed to determine whether it meets the shifting conditions for IMFs. If it does, then the analysis proceeds to the next step; otherwise, steps (2) through (4) are repeated.

6. The decomposition results from step (4) are taken as the i-th IMF component.

7. A judgment is made to determine whether the stopping criterion has been met. If so, the algorithm proceeds to step (9); otherwise, it proceeds to step (8).

8. The i-th IMF component of the original signal is used as the new original signal for step (2), and the (i+1)-th IMF component is calculated.

9. The IMF components and the residual component are obtained.

10. The number of local extremes in each IMF is counted.

11. The evaluation parameter is calculated using eq. (19):

$$f = \sum_{i=1,2,L,n} (N_{max,i} + N_{min,i})/L \quad , \quad |N_{max,i}| \geq \lambda, \; |N_{min,i}| \geq \lambda, \qquad (19)$$

where L is the frequency of the amplitude spectra; $N_{max,i}$ and $N_{min,i}$ are the numbers of local maximum and minimum, respectively, and λ is a threshold that represents the lowest energy of the local extremes in each IMF component. The threshold reflects the difference in energy before and after time-varying deconvolution. Thus, the proposed method is effective for evaluating extracted wavelets regardless of whether the wavelets are subjected to deconvolution or reflectivity inversion. This method therefore overcomes the disadvantages of conventional methods.

As discussed above, the F parameter is the number of local extremes. Greater F values correspond to more accurate extracted time-varying seismic wavelets. The evaluation indexes for the proposed method and for the parsimony and kurtosis criteria are summarized in Table 1.

Table 1. The evaluation indexes for three wavelet evaluation methods

Evaluation method	Evaluation index
EMD method	Bandwidth and energy of the amplitude spectra resulting from deconvolution or inversion.
Kurtosis criterion	Time-domain numerical characteristics of the results of reflectivity inversion.
Parsimony criterion	Time-domain numerical characteristics of the results of reflectivity inversion.

Analysis of anti-noise performance

The signal-to-noise ratios (SNRs) in real field data are low. Although noise is suppressed in pre-stack processing, it is difficult to identify and completely suppress certain types of low-energy noise; thus, random noise that is uniformly distributed throughout the frequency band at low energy is still present in post-stack seismic data. In the presence of noise, eq. (1) can be expressed as follows:

$$x(t) = \omega(t,\tau) * r(t) + v(n) \quad , \tag{20}$$

where v(n) represents random noise.

The amplitude spectrum of a seismogram is a band-limited signal; therefore, random noise can affect the high-frequency portion of the amplitude spectrum and the accuracy of the wavelets extracted via time-frequency spectral modeling. The reflectivity inversion of a time-varying wavelet extracted in the presence of noise is performed as shown in eq. (21):

$$\tilde{r}(t) = \tilde{\omega}(\tau,t) * \omega(\tau,t) * r(t) + \tilde{\omega}(\tau,t) * v(n) \quad . \tag{21}$$

When the wavelet is affected by noise, discrepancies arise between the extracted and theoretical wavelets; thus, the wavelet cannot be completely

suppressed after inversion and the degree of frequency-band broadening is limited. Moreover, a noise component exists in both the time and frequency domains of the inversion results. In the proposed EMD-based evaluation method based, which targets the frequency-domain results of either deconvolution or inversion, the influence of noise on the number of local extremes in the EMD results can be reduced by setting the lowest energies of the local extremes in each IMF.

ANALYSIS OF SIMULATION RESULTS

The original mixed-phase wavelet that was used in this experiment can be expressed using the ARMA formula as follows:

$$x(t) - 4.02x(t-1) + 8.43x(t-2) - 8.15x(t-3) + 2.86x(t-4)$$
$$= r(t) - 0.8r(t-1) + 0.2r(t-2) - 0.82r(t-3) \quad . \tag{22}$$

The equivalent of this eq. in the z domain is

$$W(z) = [1 - 0.8z^{-1} + 0.2z^{-2} - 0.82z^{-3}]$$
$$/[1 - 4.02z^{-1} + 8.43z^{-2} - 8.15z^{-3} + 2.86z^{-4}] \quad . \tag{23}$$

Fig. 2a shows the original mixed-phase wavelet, and Fig. 2b presents the corresponding reflectivity sequence, which satisfies the assumptions of independence and identical distribution (IID) and follows a Bernoulli-Gaussian distribution. The sampling interval is 1 ms. Fig. 2c shows a non-stationary seismogram that was synthesized using this time-varying wavelet and reflectivity sequence using the non-stationary convolutional model expressed in eq. (1).

Time-varying wavelet extraction

After the seismogram shown in Fig. 2c was transformed into the time-frequency domain using the improved generalized S-transform method, the seismic wavelets were extracted at every instant by applying spectral modeling in the time-frequency domain. Fig. 3 compares the extracted wavelets with the theoretical wavelets at 196 ms, 413 ms, 651 ms and 805 ms. As shown in Fig. 3, the extracted wavelets are consistent with the theoretical wavelets. Over time, the amplitude energy of the extracted wavelets decreases, reflecting the dynamic attenuation of the wavelet during propagation. These results illustrate that the time-frequency spectral modeling method can accurately extract time-varying seismic wavelets in the absence of noise.

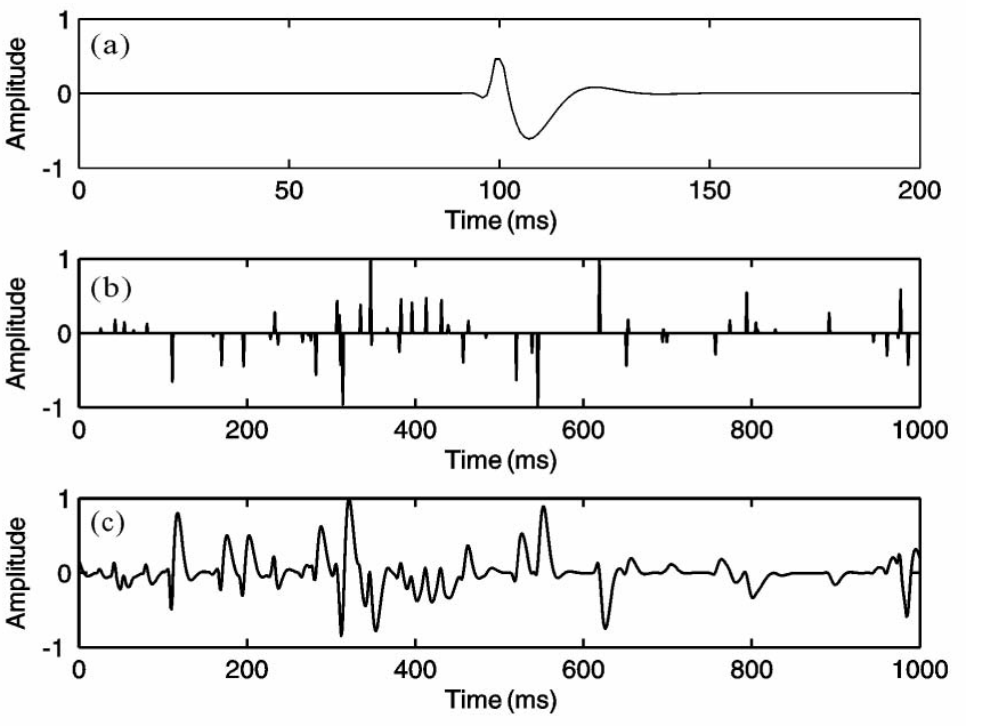

Fig. 2. Synthetic seismogram. (a) Mixed-phase wavelet; (b) Reflectivity sequence; (c) Non-stationary seismogram.

Time-varying deconvolution and reflectivity inversion

The extracted wavelets were subjected to time-varying deconvolution based on eq. (11) to suppress their time-varying nature and compensate for the observed energy attenuation; they were also subjected to reflectivity inversion by combining eq. (11) with eq. (17). The simulation results are shown in Fig.4.

By comparing Fig. 4(b) with 4(c) and Fig. 4(f) with 4(g), it can be seen that the non-stationary nature of the seismogram is suppressed and the amplitude energy is improved after time-varying deconvolution of the extracted wavelets. From Fig. 4(a) and 4(d), we know that the reflectivity sequence can be accurately inverted from the extracted wavelets. As seen from a comparative analysis of Fig. 4(e), 4(f) and 4(h), the frequency bandwidth of the seismogram has been effectively broadened after reflectivity inversion and is essentially consistent with the theoretical values. These experimental results demonstrate the validity of the time-frequency spectral model in the absence of noise.

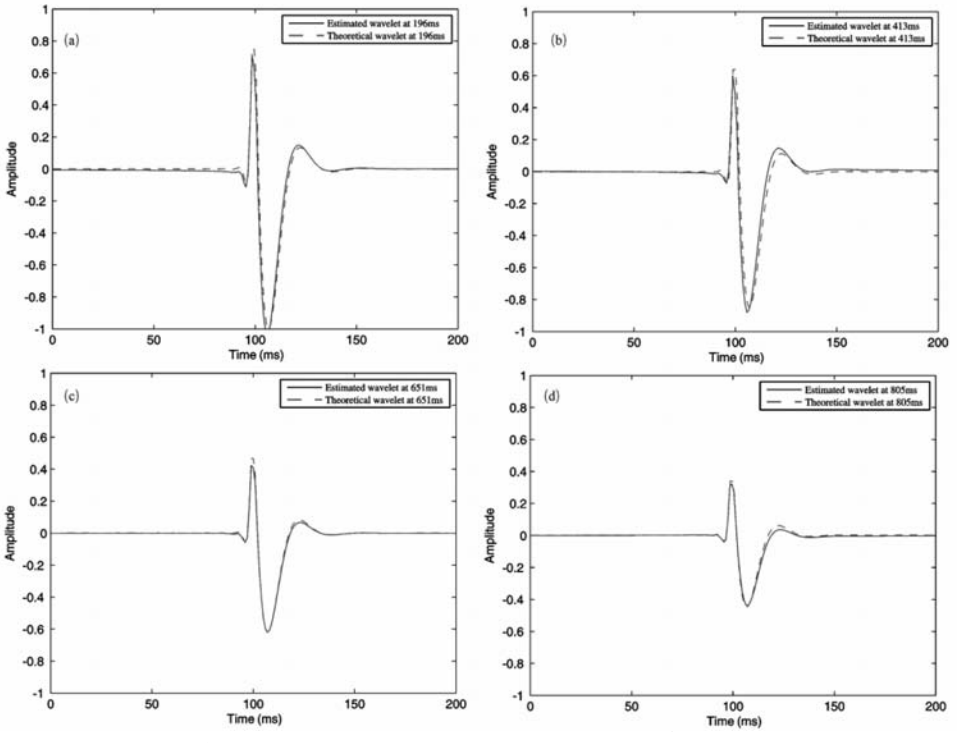

Fig. 3. Time-varying wavelet extraction results. (a) Extracted wavelet compared with the theoretical wavelet at 196 ms; (b) Extracted wavelet compared with the theoretical wavelet at 413 ms; (c) Extracted wavelet compared with the theoretical wavelet at 651 ms; (d) Extracted wavelet compared with the theoretical wavelet at 805 ms.

Evaluation of the accuracy of the extracted wavelets

Fig. 5 shows the results of applying EMD decomposition to the deconvolution and reflectivity inversion results presented in Fig. 4(f) and 4(g). The proposed method allows the evaluation of the wavelet accuracy based on the amplitude energy and bandwidth of the deconvolution or inversion results by counting the number of local extremes in each IMF.

The results of evaluating the amplitude spectra presented in Fig. 4 (e)-(h) using the proposed method were also compared with those obtained using the kurtosis and parsimony criteria (Longbottom, 1988; White, 1988), which can be expressed by eqs. (24) and (25):

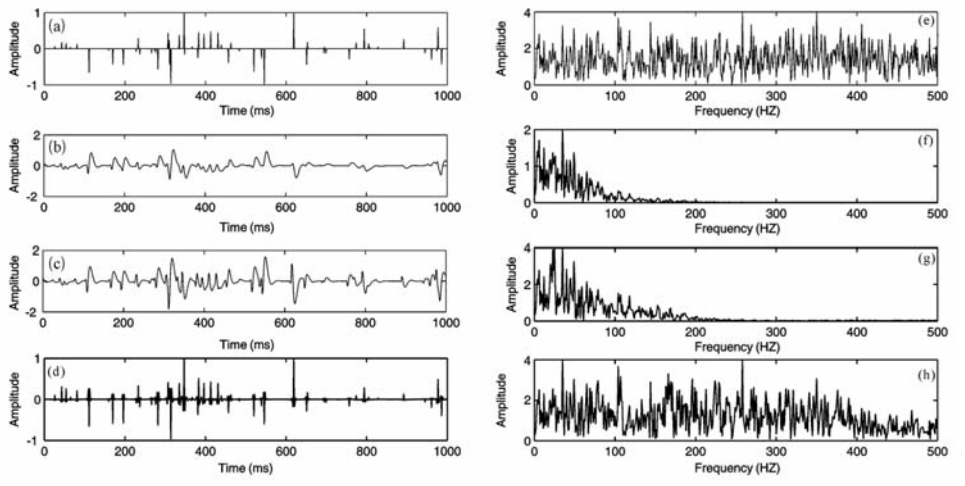

Fig. 4. Results of deconvolution and reflectivity inversion. (a) Reflectivity sequence; (b) Non-stationary seismogram; (c) Deconvolution result; (d) Reflectivity inversion result; (e) The amplitude spectrum of (a); (f) The amplitude spectrum of (b); (f) The amplitude spectrum of (c); (g) The amplitude spectrum of (d).

$$V = [\sum_{n=1}^{N} x^4(n)]/[\sum_{n=1}^{N} x^2(n)]^2 \quad , \tag{24}$$

$$P = \ln[\sum_{n=1}^{N} |x(n)|^m] - \sum_{n=1}^{N} [|x(n)|^m \cdot \ln|x(n)|^m] / \sum_{n=1}^{N} |x(n)|^m \quad , \tag{25}$$

where x(n) is the deconvolution result, $m > 2$, and N is the length of the seismogram. In these methods, the best performance is indicated when V is at a maximum and P is at a minimum. As we can observe from eqs. (19), (24) and (25), greater F and V values and smaller P values correspond to more accurate extracted wavelets. As shown in Table 2, which presents the evaluation results, all three methods are effective in the case of reflectivity inversion. However, when the wavelets are subjected to time-varying deconvolution to suppress their time-varying nature and compensate for energy attenuation, although the proposed method remains valid, the evaluation capabilities of the kurtosis and parsimony criteria decrease. Thus, the proposed EMD-based evaluation method is more effective in evaluating the bandwidth and energy in the frequency domain than conventional methods are.

Table 2. Quantitative evaluation results for all three methods in the absence of noise.

Evaluation method	Evaluation index	Original reflectivity sequence	Non-stationary seismogram	Deconvolution result	Inversion result
EMD method	F	3.1060	0.6840	1.3020	2.8720
Kurtosis criterion	V	0.0642	0.0074	0.0064	0.0508
Parsimony criterion	P	2.6299	4.4511	4.9194	2.8425

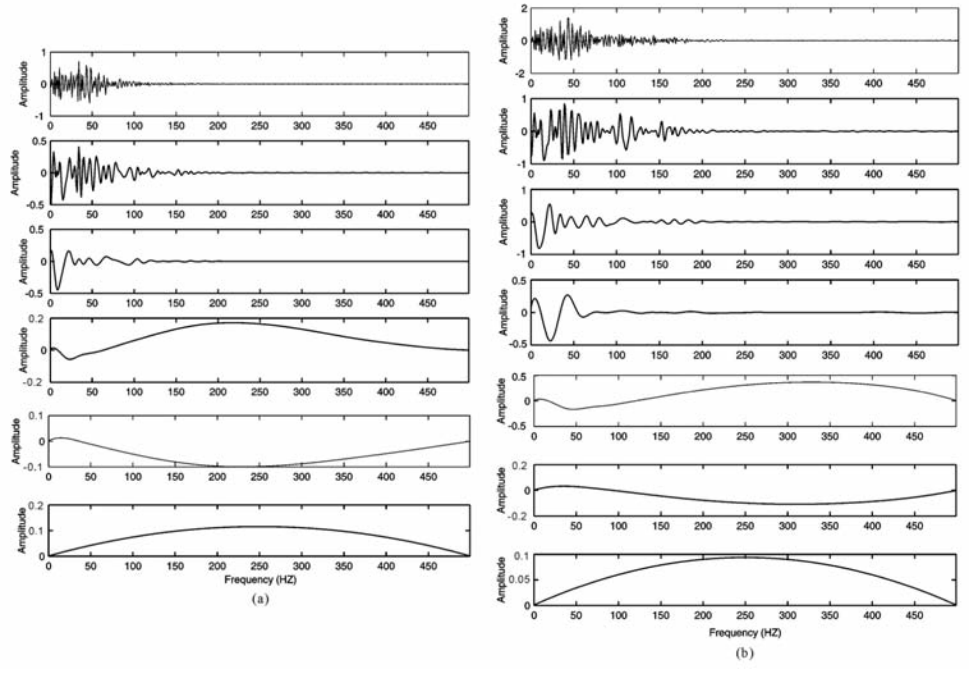

Fig. 5. EMD decomposition results. (a) EMD decomposition of Fig. 4(f); (b) EMD decomposition of Fig. 4(g).

Test of anti-noise performance

Random noise affects the accuracy of wavelet extraction and the results of deconvolution and inversion. According to eq. (16), noise is still present in a seismogram after wavelet extraction and deconvolution or reflectivity

inversion. Because the theoretical reflectivity sequence was known in this simulation, we could verify the validity of the method based on the similarity coefficient between the inverted and theoretical values. The reflectivity inversion results are shown in Figs. 6-9 for SNRs of 10 dB, 5 dB, 2 dB and 0 dB, respectively, and the corresponding quantitative evaluation results are shown in Tables 3-6.

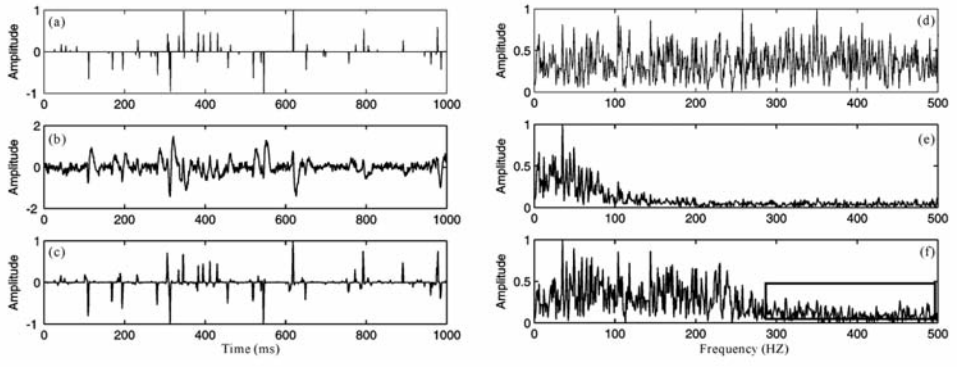

Fig. 6. Simulation results for an SNR of 10 dB. (a) Original reflectivity sequence; (b) Seismogram for an SNR of 10 dB; (c) Result of reflectivity inversion; (d) Amplitude spectrum of (a); (e) Amplitude spectrum of (b); (f) Amplitude spectrum of (c), where the portion inside the rectangle is the noise component.

Table 3-1. Quantitative evaluation result by using proposed method when the SNR is 10 dB.

Evaluation method	Original reflectivity sequence (F1)	Non-stationary seismogram (F2)	Inversion result (F3)	F3/F1	Similarity between inverted and theoretical values
EMD	3.1060	0.6720	1.6460	0.530	0.518

Table 3-2. Quantitative evaluation result by using Kurtosis criterion when the SNR is 10 dB.

Evaluation method	Original reflectivity sequence (V1)	Non-stationary seismogram (V2)	Inversion result (V3)	V3/V1	Similarity between inverted and theoretical values
Kurtosis criterion	0.0642	0.0064	0.0408	0.735	0.518

Table 3-3. Quantitative evaluation result by using Parsimony criterion when the SNR is 10 dB1.

Evaluation method	Original reflectivity sequence (P1)	Non-stationary seismogram (P2)	Inversion result (P3)	P1/P3	Similarity between inverted and theoretical values
Parsimony criterion	2.6299	8.8735	3.0315	0.867	0.518

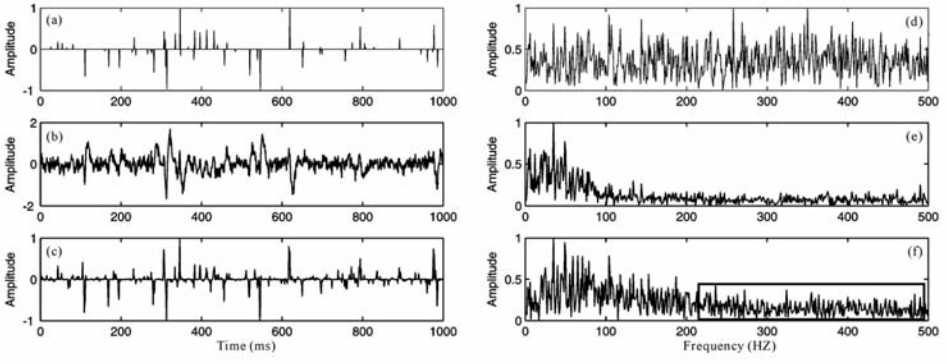

Fig. 7. Simulation results for an SNR of 5 dB. (a) Original reflectivity sequence; (b) Seismogram for an SNR of 5 dB; (c) Result of reflectivity inversion; (d) Amplitude spectrum of (a); (e) Amplitude spectrum of (b); (f) Amplitude spectrum of (c), where the portion inside the rectangle is the noise component.

Table 4-1. Quantitative evaluation result by using proposed method when the SNR is 5 dB.

Evaluation method	Original reflectivity sequence (F1)	Non-stationary seismogram (F2)	Inversion result (F3)	F3/F1	Similarity between inverted and theoretical values
EMD	3.1060	0.6640	1.3040	0.420	0.402

Table 4-2. Quantitative evaluation result by using Kurtosis criterion when the SNR is 5 dB.

Evaluation method	Original reflectivity sequence (V1)	Non-stationary seismogram (V2)	Inversion result (V3)	V3/V1	Similarity between inverted and theoretical values
Kurtosis criterion	0.0642	0.0053	0.0338	0.526	0.420

Table 4-3. Quantitative evaluation result by using Parsimony criterion when the SNR is 5 dB.

Evaluation method	Original reflectivity sequence (P1)	Non-stationary seismogram (P2)	Inversion result (P3)	P1/P3	Similarity between inverted and theoretical values
Parsimony criterion	2.6299	5.0563	3.3393	0.788	0.420

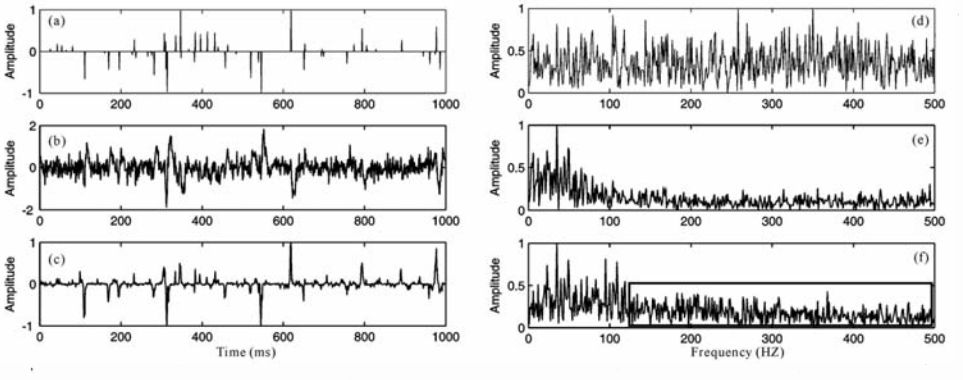

Fig. 8. Simulation results for an SNR of 2 dB. (a) Original reflectivity sequence; (b) Seismogram for an SNR of 2 dB; (c) Result of reflectivity inversion; (d) Amplitude spectrum of (a); (e) Amplitude spectrum of (b); (f) Amplitude spectrum of (c), where the portion inside the rectangle is the noise component.

Table 5-1. Quantitative evaluation result by using proposed method when the SNR is 2 dB.

Evaluation method	Original reflectivity sequence (F1)	Non-stationary seismogram (F2)	Inversion result (F3)	F3/F1	Similarity between inverted and theoretical values
EMD	3.1060	0.6420	0.8280	0.258	0.265

Table 5-2. Quantitative evaluation result by using Kurtosis criterion when the SNR is 2 dB.

Evaluation method	Original reflectivity sequence (V1)	Non-stationary seismogram (V2)	Inversion result (V3)	V3/V1	Similarity between inverted and theoretical values
Kurtosis criterion	0.0642	0.0042	0.0208	0.324	0.265

Table 5-3. Quantitative evaluation result by using Parsimony criterion when the SNR is 2 dB.

Evaluation method	Original reflectivity sequence (P1)	Non-stationary seismogram (P2)	Inversion result (P3)	P1/P3	Similarity between inverted and theoretical values
Parsimony criterion	2.6299	5.3182	3.7572	0.699	0.265

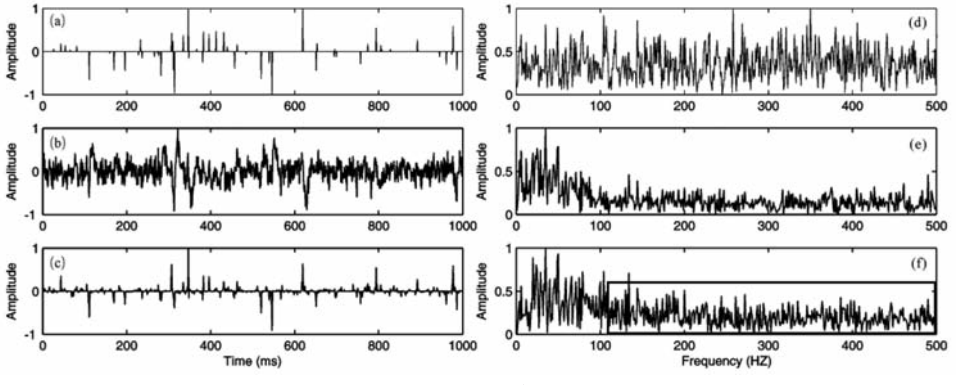

Fig. 9. Simulation result when the SNR is 0 dB. (a) Original reflectivity sequence; (b) Seismogram when SNR is 0 dB; (c) Result of reflectivity inversion; (d) Amplitude spectra of (a); (e) Amplitude spectra of (b); (f) Amplitude spectra of (c) , where the rectangular part is the noise component.

Table 6-1. Quantitative evaluation result by using proposed method when the SNR is 0 dB.

Evaluation method	Original reflectivity sequence (F1)	Non-stationary seismogram (F2)	Inversion result (F3)	F3/F1	Similarity between inverted and theoretical values
EMD	3.1060	0.6720	0.7210	0.232	0.224

Table 6-2. Quantitative evaluation result by using Kurtosis criterion when the SNR is 0 dB.

Evaluation method	Original reflectivity sequence (V1)	Non-stationary seismogram (V2)	Inversion result (V3)	V3/V1	Similarity between inverted and theoretical values
Kurtosis criterion	0.0642	0.0039	0.0174	0.271	0.224

Table 6-3. Quantitative evaluation result by using Parsimony criterion when the SNR is 0 dB.

Evaluation method	Original reflectivity sequence (P1)	Non-stationary seismogram (P2)	Inversion result (P3)	P1/P3	Similarity between inverted and theoretical values
Parsimony criterion	2.6299	5.4701	4.1236	0.638	0.224

As shown in the above tests, the proposed EMD-based method can be used to objectively evaluate the accuracy of extracted wavelets under various SNR conditions, and it is more accurate and stable than conventional evaluation criteria. The quantitative evaluation results in the presence of noise indicate that the accuracy of time-varying wavelet extraction based on time-frequency spectral modeling is affected by noise; as the noise increases, the wavelet extraction accuracy degrades. This conclusion is consistent with the theoretical analysis.

ANALYSIS OF REAL SEISMIC DATA

Fig. 10 shows the post-stack seismic section of an oil field obtained using a sampling interval of 1 ms. The validity of the proposed method for the processing of actual seismic data was verified using the workflow illustrated in Fig. 1.

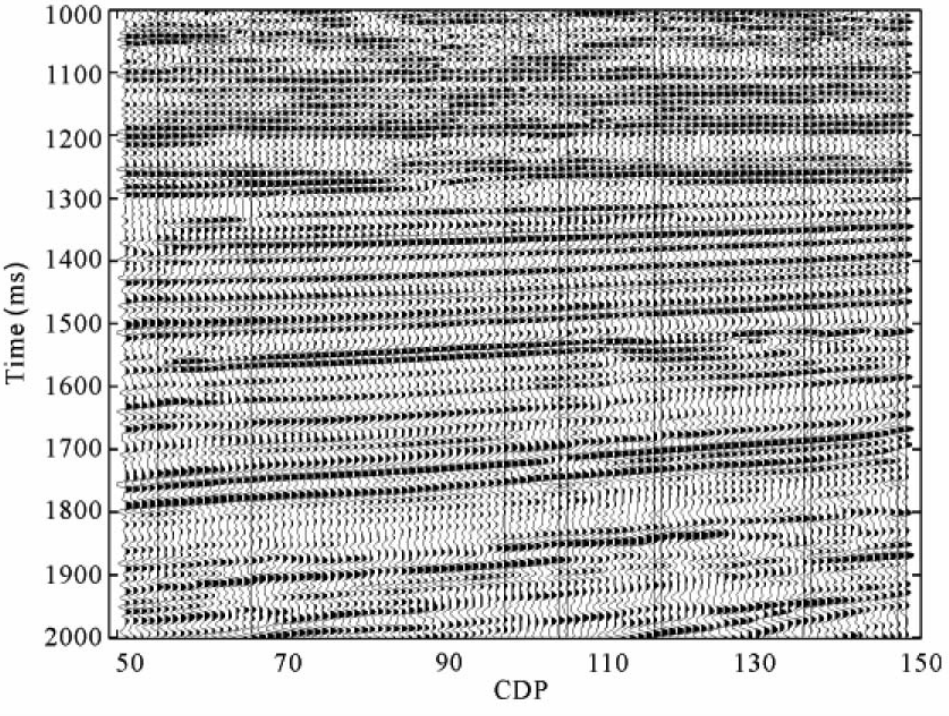

Fig. 10. Actual post-stack seismic section of an oil field.

Single trace test

The 131st trace, which is shown in Fig. 11 (a), was considered as an example. The time-varying seismic wavelets were extracted via time-frequency spectrum modeling at, for example, 1.2 s, 1.5 s and 1.8 s, as shown in Fig. 11(b), and the results were found to exhibit the expected dynamic attenuation due to absorption.

Fig. 12 shows the comparison against a well log synthetic with the reflectivity inversion result obtained from the extracted wavelets. The proposed method and the kurtosis and parsimony criteria were used to evaluate the results presented in Fig. 12, and the evaluation results are shown in Table 7. As seen from Table 7, the evaluation result by using proposed method is closest to the similarity between the inverted and logging values and we conclude that the proposed EMD-based method is more effective and accurate than the conventional methods, which is consistent with the conclusions obtained from the theoretical analyses and numerical simulations.

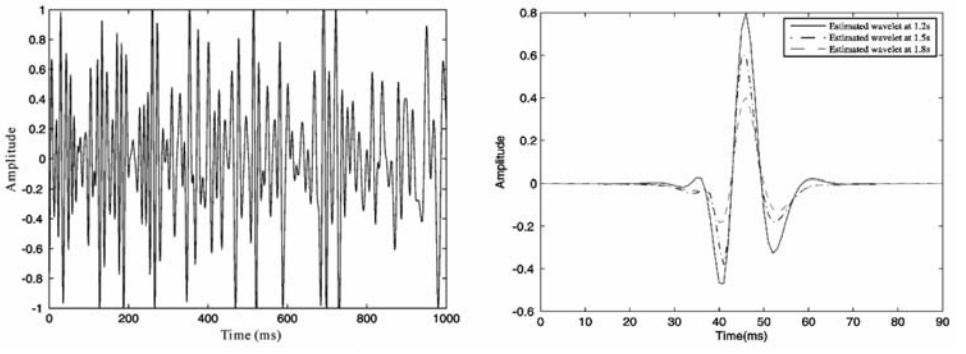

Fig. 11. Time-varying wavelet extraction from actual seismic data. (a) The 131st seismic trace; (b) Wavelets extracted via time-frequency spectral modeling.

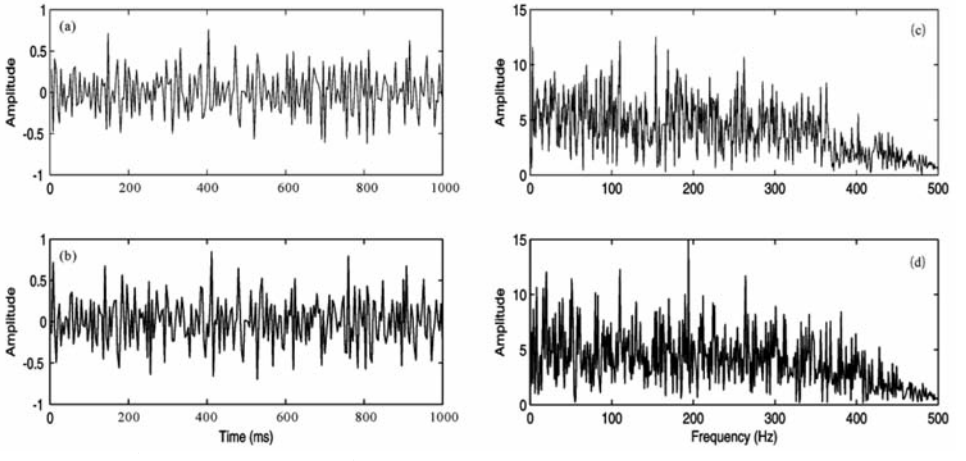

Fig. 12. The comparison against a well log synthetic with the reflectivity inversion result (a) Reflectivity inversion result; (b) Reflectivity from logging; (c) Amplitude spectrum of (a); (d) Amplitude spectrum of (b)

Table 7-1. Quantitative evaluation result for actual seismic data by using proposed method.

Evaluation method	Reflectivity from logging (F1)	Reflectivity inversion result (F2)	F2/F1	Similarity between the inverted and logging values
EMD	3.3420	3.0060	0.899	0.876

Table 7-2. Quantitative evaluation result for actual seismic data by using Kurtosis criterion.

Evaluation method	Reflectivity from logging (V1)	Reflectivity inversion result (V2)	V2/V1	Similarity between the inverted and logging values
Kurtosis criterion	0.0086	0.0079	0.918	0.876

Table 7-3. Quantitative evaluation result for actual seismic data by using Parsimony criterion.

Evaluation method	Reflectivity from logging (P1)	Reflectivity inversion result (P2)	P1/P2	Similarity between the inverted and logging values
Parsimony criterion	5.0488	5.4902	0.920	0.876

Multi-trace seismic data test

To further verify the practicability of the proposed method, the multi-trace seismic data was deconvolved using the extracted wavelets, as shown in Fig. 13. Fig. 13 reveals that the seismic data after deconvolution is of higher resolution. Fig. 14 describes the frequency-domain results of Fig. 13, and it is shown that the bandwidth and amplitude energy are improved after deconvolution. Thus, it is concluded that time-varying wavelet extraction can be applied to improve the resolution of seismic data.

The quantitative evaluation results for the processing of the multi-trace seismic data are shown in Table 8. These evaluation results also indicate that time-frequency spectral modeling can help to broaden the bandwidth and improve the resolution of seismic data.

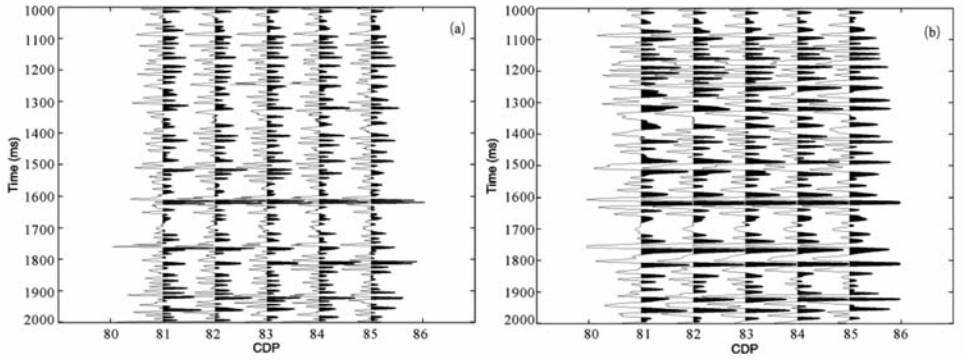

Fig. 13. Deconvolution results for the multi-trace seismic data. (a) Seismic data before deconvolution; (b) Seismic data after deconvolution.

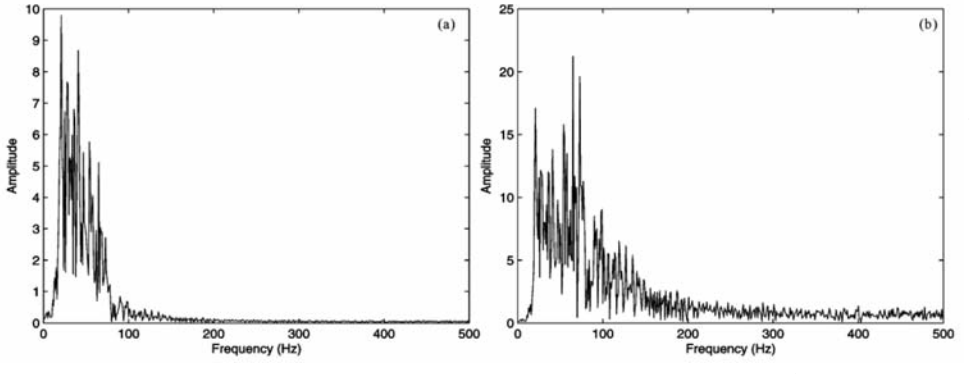

Fig. 14. Amplitude spectra of Fig. 13. (a) Amplitude spectrum of Fig.13(a); (b) Amplitude spectrum of Fig. 13(b).

Table 8. Quantitative evaluation results for the multi-trace seismic data.

Evaluation method	Evaluation index	Original seismic data	Seismic data after deconvolution
EMD	F	1.1879	1.8326

CONCLUSION

In this paper, a quantitative evaluation method based on EMD for determining the accuracy of time-varying seismic wavelet extraction is proposed. Theoretical analyses, numerical simulations and the results of processing real data verify that the proposed method can be applied to quantitatively evaluate the accuracy of extracted time-varying wavelets. The study yields the following conclusions:

1. The proposed method is more effective and intuitive than conventional qualitative evaluations, overcomes the deficiencies of conventional evaluation criteria in evaluating the bandwidth and energy in the frequency domain, and enables a quantitative evaluation of wavelet accuracy based on the results of time-varying deconvolution and reflectivity inversion. The proposed method facilitates the selection and application of an accurate time-varying wavelet extraction method in seismic data processing. Moreover, the method can be used to obtain accurate evaluations in the presence of noise.

2. Time-varying seismic wavelet extraction based on time-frequency spectral modeling is precise in the absence of noise but is easily corrupted by noise. More specifically, the validity of the method is degraded in noisy environments. Therefore, the improvement of existing methods of time-varying wavelet extraction or the development of novel methods with better anti-noise capabilities is expected to be a popular area of research in the future.

ACKNOWLEDGMENT

This research was supported by the National Natural Science Foundation of China (40974072). The authors gratefully acknowledge this financial support.

REFERENCES

Arild, B. and Henning, O., 2003. Bayesian wavelet estimation from seismic and well data. Geophysics, 68: 2000-2009. doi: 10.1190/1.1635053

Chen, J., Dai, Y.S., Zhang, Y.N., Wei, Y.Q. and Ding, J.J., 2013. Summary of the evaluation approaches for seismic wavelet pick-up based on higher order statistics. Oil Geophys. Prosp., 48: 497-503. doi:10.13810/j.cnki.issn.1000-7210.2013.03.024.

Dai, Y.S., Zhang, M.M., Zhang, Y.N., Ding, J.J. and Wang, R.R., 2015. Time-variant mixed-phase seismic wavelet estimation based on spectral modeling in the time-frequency domain. Oil Geophys. Prosp., 50: 830-838. doi:10.13810/j.cnki.issn.1000-7210.2015.05.004.

Economou, N. and Vafidis, A., 2010. Spectral balancing GPR data using time-variant bandwidth in the t-f domain. Geophysics, 75: J19-J27. doi:10.1190/1.3374464.

Han, J. and van der Baan, M., 2013. Empirical mode decomposition for seismic time-frequency analysis. Geophysics, 78: O9-O19. doi:10.1190/geo2012-0199.1.

Huang, N.E., Shen, Z., Long, S.R., Wu, M.C., Shih, H.H., Zheng, Q.A., Yen, N.C., Tung, C.C. and Liu, H.H., 1998. The empirical mode decomposition and the Hilbert spectrum for nonlinear and non-stationary time series analysis. Proc. Roy. Soc. Mathemat., Phys. Engineer. Sci., 454: 903-995. doi:10.1098/rspa.1998.0193.

Li, G.F., Liu, Y., Zheng, H. and Huang, W., 2015. Absorption decomposition and compensation via a two-step schem. Geophysics, 80: V145-V155. doi:10.1190/geo2015-0038.1.

Longbottom, J., Walden, A.T. and White, R.E., 1988. Principles and application of maximum Kurtosis phase estimation. Geophys. Prosp., 36: 115-138. doi:10.1111/j.1365-2478.1988.tb02155.x.

Margrave, G.F., Lamoureux, M.P. and Henley, D.C., 2011. Gabor deconvolution: Estimating reflectivity by nonstationary deconvolution of seismic data. Geophysics, 76: W15-W30. doi:10.1190/1.3560167.

Matsuoka, T. and Ulrych, T.J., 1984. Phase estimation using the bispectrum: Proc. IEEE, 72: 1403-1411. doi:10.1109/PROC.1984.13027.

Oliveira, S.A.M. and Lupinacci, W.M., 2013. L_1-norm inversion method for deconvolution in attenuating media. Geophys. Prosp., 61: 771-777. doi:10.1111/1365-2478.12002.

Porsani, M.J., Ursin, B. and Silva, M.G., 2013. Dynamic estimation of reflectivity by minimum-delay seismic trace decomposition. Geophysics, 78: V109-V117. doi:10.1190/geo2012-0077.1.

Radad, M., Gholami, A. and Siahkoohi, H.R., 2015. S-transform with maximum energy concentration: Application to non-stationary seismic deconvolution. J. Appl. Geophys., 118: 155-166. doi:10.1016/j.jappgeo.2015.04.010.

Rietsch, E., 1997. Euclid and the art of wavelet estimation, Part I: Basic algorithm for noise-free data. Geophysics, 62: 1931-1938. doi:10.1190/1.1444293.

Rosa, A.L. and Ulrych, T.J., 1991. Processing via spectral modeling. Geophysics, 56: 1244-1251. doi:10.1190/1.1443144.

Sajid, M. and Ghosh, D., 2013. A fast and simple method of spectral enhancement. Geophysics, 79: V75-V80. doi:10.1190/geo2013-0179.1.

Sun, X.K., Sun Z.D., Xie, H.W., Liu, L.F., Tao, P. and Wang, Y.G., 2015. A nonstationary perspective on sparse deconvolution. Oil Geophys. Prosp., 50: 260-266. doi:10.13810/j.cnki.issn.1000-7210.2015.02.009.

van der Baan, M., 2008. Time-varying wavelet estimation and deconvolution by Kurtosis maximization. Geophysics, 73: 11-18. doi:10.1190/1.2831936.

Velis, D.R., 2008. Stochastic sparse-spike deconvolution. Geophysics, 73: R1-R9. doi:10.1190/1.2790584.

Wang, L.L., Gao, J.H., Zhao, W. and Jiang, X., 2012. Enhancing resolution of nonstationary seismic data by molecular-Gabor transform. Geophysics, 78: V31-V34. doi:10.1190/geo2011-0450.1.

White, R.E., 1988. Maximum Kurtosis phase correction. Geophys. J., 95: 371-389. doi: 10.1111/j.1365-246X.1988.tb00475.x.

Yuan, S.Y. and Wang, S.X., 2011. Influence of inaccurate wavelet phase estimation on seismic inversion. Appl. Geophys., 8: 48-59. doi:10.1007/s11770-011-0273-5.

Zhang, G., Li, Y., Rong, J. and Cai, Z., 2011. Compensation for stratigraphic absorption of seismic attenuation based on the improved generalized S-transform. Extended Abstr., 73rd EAGE Conf., Vienna. doi:10.3997/2214-4609.20149195.

Zhou, H.L., Tian, Y.M. and Ye, Y., 2014. Dynamic deconvolution of seismic data based on generalized S-transform. J. Appl. Geophys., 108: 1-11. doi:10.1016/j.jappgeo.2014.06.004.